Exploration of biomarkers of psoriasis through combined multiomics analysis

Lu Xing
Kunming Children's Hospital
Li Yu
Kunming Children's Hospital
Nian Zhou
Kunming Children's Hospital
Zhao Zhang
Kunming Children's Hospital
Yunjing Pu
Kunming Children's Hospital
Jingnan Wu
Kunming Children's Hospital
Hong Shu (pfk2145@126.com)
Kunming Children'S Hospital https://orcid.org/0000-0002-5037-7557

Research Article

Keywords: DNA methylation, Psoriasis, Diagnostics, Indicators, Bioinformatics, Machine learning

Posted Date: April 6th, 2022

DOI: https://doi.org/10.21203/rs.3.rs-1507834/v1

Title

Exploration of biomarkers of psoriasis through combined multiomics analysis

Authors'Information

1.Lu Xing (the Lead author), 914760716@qq.com**,** Department of dermatology, Children's Hospital Affiliated to Kunming Medical University, Kunming Children's Hospital, China
2.Li Yu, 422811194@qq.com, Department of dermatology, Children's Hospital Affiliated to Kunming Medical University, Kunming Children's Hospital, China
3.Nian Zhou, 418198266@qq.com, Department of dermatology, Children's Hospital Affiliated to Kunming Medical University, Kunming children's Hospital, China
4.Zhao Zhang, sky1314andy@163.com, Department of dermatology, Children's Hospital Affiliated to Kunming Medical University, Kunming Children's Hospital, China
5.Yunjing Pu, 942687928@qq.com, Department of dermatology, Children's Hospital Affiliated to Kunming Medical University, Kunming Children's Hospital, China
6.Jingnan Wu, wujingnan0704@sina.com, Department of dermatology, Children's Hospital Affiliated to Kunming Medical University, Kunming Children's Hospital, China
7.**Hong Shu (Corresponding Author),** pfk2145@126.com, Department of dermatology, Children's Hospital Affiliated to Kunming Medical University, Kunming Children's Hospital, 650100, 288 Qianxing Road, Xishan District, Kunming City, Yunnan Province, China

Exploration of biomarkers of psoriasis through combined multiomics analysis

Abstract

Background: Aberrant DNA methylation patterns are of increasing interest in the study of psoriasis mechanisms. This study aims to screen potential diagnostic indicators affected by DNA methylation for psoriasis based on bioinformatics using multiple machine learning algorithms and to preliminarily explore its molecular mechanisms.

Methods: GSE13355, GSE14905, and GSE73894 were collected from the gene expression omnibus (GEO) database. Differentially expressed genes (DEGs) and differentially methylated region (DMR)-genes between psoriasis and control samples were combined to obtain differentially expressed methylated genes. Subsequently, protein-protein interaction (PPI) network establishment, multiple machine learning algorithm analysis, including, the least absolute shrinkage and selection operator (LASSO), Random Forest (RF), and Support Vector Machine (SVM), receiver operating characteristic (ROC) curve analysis, and single-gene gene set enrichment analysis (GSEA) were performed to analyze the interaction networks, to recognize hub genes, and to clarify the pathogenesis of psoriasis. The druggable genes were predicted using DGIdb. The expression of GJB2 in psoriasis lesions and healthy controls was detected by immunohistochemistry (IHC) and quantitative real-time PCR(RT-qPCR).

Results: In this study, a total of 767 DEGs and 896 DMR-genes were obtained. Functional enrichment showed that they were significantly associated with skin development, skin barrier function, immune/inflammatory response, and cell cycle. The combined transcriptomic and DNA methylation data resulted in 33 differentially expressed methylated genes, of which The gap junction beta 2 (GJB2) was the final identified hub gene for psoriasis, with the robust diagnostic power. IHC and RT-qPCR showed that GJB2 was significant higher in psoriasis than that in healthy controls. Single gene GSEA suggested that GJB2 may be involved in the development and progression of psoriasis by disrupting the body's immune system, mediating the cell cycle, and destroying the skin barrier, in addition to possibly inducing diseases related to the skeletal aspects of psoriasis. Moreover, OCTANOL and CARBENOXOLONE were identified as promising compounds through the DGIdb database.

Conclusion: Our findings suggest that the abnormal expression of GJB2 may play a critical role in psoriasis development and progression. The genes identified in our study may serve as a diagnostic indicator and therapeutic target in psoriasis.

Keyword: DNA methylation; Psoriasis; Diagnostics; Indicators; Bioinformatics; Machine learning

1. Introduction

Psoriasis is a chronic recurrent inflammatory skin disease induced by the interaction of heredity and environment. The typical clinical manifestation is scaly erythema or plaque, which is localized or widely distributed [1]. The incidence of psoriasis in developed countries is higher than that in developing countries, and that in children is lower than that in adults [2,3]. The prevalence of psoriasis is the same in men and women, with an average age of about 33 years [4]. At present, the therapeutic drugs for psoriasis are particularly diverse, such as retinoids, immunosuppressants, glucocorticoids, and biological agents. However, psoriasis is remained incurable, which showed a high recurrence rate after drug withdrawal [5,6]. Biological agents have greatly changed the treatment and management of psoriasis due to their high efficiency and few side effects [7], but psoriasis patients with hepatitis B, tuberculosis, and allergies are not suitable for biologics [8-10]. The pathogenesis of psoriasis is not completely clear, but more and more evidence show that abnormal DNA methylation pattern is one of the most critical pathogenic factors, including differential methylation sites and differential methylation regions [11-13].

DNA methylation, an epigenetic regulatory mechanism, plays essential roles in gene expression, differentiation, cell proliferation, development, and genomic imprinting [14,15]. It's mediated by DNA methyltransferase, which occurs on cytosine phosphate guanine (CPG) island and transfers the methyl of S-adenosylmethionine to the 5th carbon atom of the cytosine ring [16]. DNA methylation is generally negatively correlated with gene expression [17]. Several studies have demonstrated that DNA methylation was closely related to the pathogenesis, severity, and treatment of psoriasis. The down-regulation of secreted frizzled-related protein 4 (SFRP4) caused by hypermethylation [18] or the up-regulation of B-cell receptor-associated protein 31 (BACP31) caused by hypomethylation [19] might lead to excessive proliferation and abnormal apoptosis of psoriasis keratinocytes. The results of genome-wide methylated DNA immunoprecipitation sequencing (MeDIP-Seq) on lesions and healthy skin of psoriasis patients showed that differential methylated regions (DMR) covered almost all genomes, and the methylation levels of tissue inhibitor of metalloproteinase 2(TIMP2) and programmed cell death 5(PDCD5) were positively correlated with the score of psoriatic area and severity index (PASI) [20]. DNA methylation spectrum analysis was performed on the genomes of 12 lesions of psoriasis patients pre-and post-ultraviolet radiation B(UVB) treatment. The results suggested that the methylation status of 3665 methylation variable positions (MVP) in psoriasis samples had changed, and the patient's condition had improved. It indicated that DNA methylation could be dynamically reversed in the treatment of psoriasis [21]. Therefore, the exploration of key genes related to DNA methylation and their biological function was extremely crucial to reveal the molecular mechanism of psoriasis and develop new therapeutic targets.

In this study, we first utilized bioinformatics to analyze the transcriptome data and methylation data of psoriatic lesions and healthy controls in the GEO database. Next, multiple machine learning algorithms are used to screen key genes related to DNA methylation and ROC curve are used to evaluate its diagnostic value in psoriasis. Finally, we verified the expression of key genes by molecular biological experiment.

In conclusion, our study performed the identification of promising diagnostic indicator and therapeutic target of psoriasis by combined multiomics analysis.

2. Materials and methods

2.1 Clinical sample collection

Eight psoriasis patients and eleven healthy controls admitted to the dermatology of Kunming Children's Hospital were enrolled in the study. Written informed consent was obtained from all participants prior to enrollment into the study. Study protocols were approved by the Ethics Committee of the Kunming Children's Hospital, based on the ethical principles for medical research involving human subjects of the Helsinki Declaration.

2.2Data source

The psoriasis-related data utilized for this study were obtained from the GEO database. Gene expression profiling array (GSE13355; https://www.ncbi.nlm.nih.gov/geo/query /acc.cgi?acc=GSE13355) [22-24] provided mRNA expression data from 122 skin biopsy samples with 58 psoriasis lesions and 64 healthy control skin. A total of 54 samples with 33 psoriasis lesions and 21 healthy control skin were obtained from the GSE14905(https://www.ncbi.nlm.nih.gov/geo/query/acc.cgi?acc=GSE14905) [25] gene expression profiling, both datasets were generated by the platform GPL570 (Affymetrix Human Genome U133 Plus 2.0 Array).

The DNA methylation MBD-seq data were obtained under accession number GEO: GSE73894 (GPL13534 platform; https://www.ncbi.nlm.nih.gov/geo/query/acc.cgi?ac c=GSE73894) [26,27], which includes 114 psoriasis lesions and 64 healthy control skin samples.

2.3 Differentially expressed genes analysis

R package limma [28] was used in differentially expressed gene (DEG) analysis. Genes with absolute $\log_2$ fold change (FC) > 1 and $P < 0.05$ were defined as DEGs.

2.4 Analysis of differentially methylated regions

The Bumphunter function of the R package ChAMP was used for the differentially methylated region (DMR) analysis. The parameter setting was as follows: a minimum number of probes in the methylation region (minProbes) ≥ 7, adjusted (adj.) $P < 0.05$. The methylation level of the gene was represented by the average beta value of CpG in different regions of the gene. The beta value matrix was analyzed by the R package limma to screen differentially methylated genes, and the $|\Delta\beta| > 0.1$ was set as the threshold. The diagram drawn by the R package named “Upset” would be used to show the distribution of genes in different gene regions [29]. The intersection of DEGs and DMR-genes was represented by differentially expressed methylated genes.

2.5 Functional enrichment analysis

Gene ontology (GO) [30]and Kyoto Encyclopedia of Genes and Genomes (KEGG) [31] pathway enrichment analysis were performed by the R package clusterProfiler [32]. $P <$ 0.05 and count > 2 were considered to be statistically significant.

2.6 Protein-protein interaction (PPI) network analysis

To explore the interaction between differentially expressed methylated genes, we uploaded these genes to the STRING database(https://string-db.org) to get the

interaction relationship information between genes, and the cutoff value was set to 0.15. Then, the interactive information was imported into Cytoscape [33] to construct a PPI network. The top 10 genes in the descending ranking were identified as key genes for subsequent analysis based on the connectivity (degree) of each node in the PPI network.

2.7 Integrating multiple machine learning algorithms to identify hub genes

Three machine learning algorithms were implemented to filter feature genes: least absolute shrinkage and selection operator (LASSO; R package glmnet), random forest classifier (RF; R package randomForest), and support vector machine recursive feature elimination (SVM-RFE; R package e1071) using a 10-fold cross-validation approach.

LASSO [34] reduces feature space dimension and filters variables by performing a penalized function that compresses insignificant coefficients to zero and therefore contracts subsets and processes data with complex collinearity. The parameters were set to famil: binomial and type.measure: class.

In the RF [35]model, the importance and importance ranking of each gene are obtained using the RFE method (iterate through the process of gradually reducing the combination of all genes to one gene combination, calculate the importance of genes in each iteration and rank them in ascending order, remove the unimportant genes, rank the remaining genes in importance, then repeat), and obtain the error rate and accuracy rate of the combination in each iteration, select the best combination with the lowest error rate, and match the corresponding gene as the characteristic gene.

SVM-RFE [36]is a sequence backward selection algorithm based on the maximum interval principle of SVM. We applied the 10-fold cross-validation algorithm as the resampling method for SVM-RFE. The final importance of features was based on the average importance of each feature in each iteration.

Afterward, we selected those within the intersection of three subsets as a hub gene for subsequent analyses.

2.8 The receiver operating characteristic (ROC) curve analysis

The receiver operating characteristic (ROC) curve analysis was used to evaluate the discrimination ability of the hub gene in the GSE13355 dataset; the discrimination ability of each model was quantified by the area under the ROC curve (AUC). The reliability of these gene predictions would be verified in the independent GSE14905 dataset. The ROC analysis was achieved through the R package pROC [37].

2.9 Single-gene gene set enrichment analysis (GSEA) analysis

Single-gene GSEA was conducted based on the gene list sorted by Spearman correlation coefficient between every gene and the specified hub gene to predict the significant biological processes and pathways associated with the hub gene. The background gene sets for GO and KEGG were obtained from the MSigDB database (https://www.gsea-msigdb.org/gsea/msigdb/). The |Normalized Enrichment Score (NES)| > 1, $P < 0.05$, and $q < 0.2$ were considered significant.

2.10 Drug and hub gene interaction analysis

The drug-gene interaction database (DGIdb; https://www.dgidb.org/) was used to investigate potential diagnosis-related gene therapy targets. The online DGIdb is a

user-friendly resource, which stores information about druggability and interactions between drugs and genes from the published literature, databases, and web resources [38].

2.11 Immunohistochemical staining

The 8 psoriasis lesions and 11 healthy skin tissues were made into paraffin blocks, which were then cut into sections at a thickness of 5μm by a slicer (Leica Co., Ltd., Shanghai, China), followed by baking at 50°C. The sections were dewaxed twice using xylene (5 min each) and then dehydrated by graded ethanol with a certain concentration, separately (3 min each). The endogenous peroxidase in the tissue sections was blocked with methanol containing 0.3% H_2O_2. The sections were then incubated with the anti-connexin 26 (Cx26) antibody (1:100, Ab65969, Abcam, Cambridge, UK) as primary antibodies at 4 ℃ was performed using the streptavidinbiotin peroxidase (SP) coupling two-step method and standard SP kit. Pathological changes were observed under an optical microscope (DMM-300D, Shanghai Caikon Optical Instrument Co., Ltd., Shanghai, China) (× 200) and photographed.

2.12 RNA isolation and quantification

The total RNA from 8 psoriasis lesions and 11 healthy skin tissues were extracted based on the Trizol method (Cat:9109, Takara, Dalian, China). Total RNA was reversely transcribed into cDNA using a reverse transcription kit (Cat: KR118-02, TianGen, Beijing, China), after which quantitative PCR (qPCR) amplification analysis was conducted. Primers of GJB2 and GAPDH were designed and then synthesized by Sangon company (Sangon Biotech, Shanghai, China) **(Table 1)**. The qPCR was subsequently conducted using the dNTP mixture (Cat: FP205-02, TianGen, Beijing, China) on the 7500 Real-Time PCR Systems (Applied Biosystems, Thermo Fisher Scientific, Foster City, California). GAPDH was regarded as the internal reference. $2^{-\Delta Ct}$ was employed to determine the expression ratio of the target gene in the psoriasis group to that of the healthy group, using the following formula: ΔCt= Ct (GJB2)–Ct (GAPDH). The experiment was independently repeated three times.

2.13 Statistical analysis

The R software packages were used in the statistical analysis. All network plots were visualized by Cytoscape software. The R package (ggplot2, Pheatmap, GOplot, UpSetR, VennDiagram, ggpubr) was used for visualization (volcano plot, heat map, GO/KEGG enrichment plot, upset plot, Venn diagram, box line plot). The difference in hub genes between normal and psoriasis samples was detected by the Wilcoxon rank-sum test. $P < 0.05$ was set as the threshold of significance if not otherwise stated.

3. Results

3.1 Analysis of the psoriasis-related DEGs in the GSE13355 dataset

After background correction and Robust Multichip Average (RAM) normalization of gene expression profiles from skin samples of 58 psoriasis patients and 64 healthy subjects in the GSE13355 dataset using the R package affy (V 1.70.0), PCA showed that the same type of samples in this dataset had aggregation properties

(Supplementary Figure 1). Then, using the R package limma, genes satisfying $|\log_2 FC| > 1$ and $P < 0.05$ were identified between psoriasis and healthy samples (psoriasis vs. healthy). A total of 767 DEGs were identified, of which 448 genes were expressed up-regulated in psoriasis samples and 319 genes were down-regulated compared to healthy control samples **(Figure 1A; Supplementary Table 1)**. The heatmap demonstrated the differential expression patterns of top 100 up- and down-regulated genes between the two groups **(Figure 1B)**.

Next, we performed functional enrichment analysis on these DEGs. GO analysis **(Figure 1C; Supplementary Table 2)** revealed that in the BP category, DEGs were significantly associated with skin development ('skin development', 'epidermis development', 'positive regulation of epidermal growth factor-activated receptor activity', 'molting cycle', 'skin epidermis development', *etc.*), viral ('response to virus', 'defense response to virus', 'viral genome replication', 'regulation of viral life cycle', *etc.*)/bacterial ('response to molecule of bacterial origin', 'defense response to fungus', 'response to fungus', *etc.*) response, immune ('antimicrobial humoral response', 'regulation of innate immune response', 'type 2 immune response', *etc.*)/inflammatory ('regulation of inflammatory response', 'response to chemokine', 'interleukin-1 beta production', *etc.*) response, and cell cycle ('organelle fission', 'regulation of chromosome segregation', 'negative regulation of mitotic sister chromatid segregation', *etc.*); also, 'cornification', 'epidermal cell differentiation', and 'keratinocyte differentiation' were also significantly enriched. Furthermore, these genes were inextricably linked to 'positive regulation of wound healing', 'establishment of skin barrier', 'regulation of response to wounding', and several physiological processes such as differentiation, migration, and chemotaxis of various immune cells (e.g., leukocytes, neutrophils, T cells, macrophages). In the CC category, cornified envelope, collagen-containing extracellular matrix, condensed chromosome, centromeric region, clathrin-coated vesicle membrane, and condensed chromosome kinetochore were the five most significantly enriched terms **(Supplementary Table 2)**. Moreover, the MF category indicated that these genes were remarkably relevant to chemokines ('chemokine activity', 'chemokine receptor binding', 'CXCR chemokine receptor binding', 'CCR chemokine receptor binding'), cytokines ('cytokine activity', 'cytokine receptor binding', 'cytokine binding'), and growth factors ('growth factor receptor binding' and 'epidermal growth factor receptor binding') **(Supplementary Table 2)**. KEGG analysis illustrated that these genes were involved in a total of 9 pathways, including those associated with cancer ('PPAR signaling pathway' and 'Prostate cancer'), viral infection ('Influenza A' and 'Hepatitis C'), and inflammatory responses ('Viral protein interaction with cytokine and cytokine receptor', 'IL-17 signaling pathway', 'Cytokine-cytokine receptor interaction', and 'Chemokine signaling pathway'). Moreover, the Pyrimidine metabolism pathway was also significantly enriched **(Figure 1D; Supplementary Table 3)**.

3.2 DNA methylation profiling of human psoriasis in the GSE73894 dataset

DNA methylation is a highly stable epigenetic mark associated with disease pathogenesis [13]. DNA methylation has been reported to be one of the important factors in the differentiation of keratin-forming cells [16,39], which prompted us to

speculate that DNA methylation is essential for the development of psoriasis. To characterize aberrant DNA methylation in psoriasis, we evaluated the overall DNA methylation levels in 64 healthy control skins and lesioned skins of psoriasis patients from the GSE73894 dataset and found relatively high methylation levels in lesioned skins of psoriasis compared to healthy control skins **(Figure 2A)**. Subsequently, the methylation data were quality-controlled and normalized by the R package ChAMP. A total of 73107 low-quality probes were filtered out from 485577 probes. PCA **(Supplementary Figure 2A)** and methylation distribution density **(Supplementary Figure 2B)** analyses based on the beta value of the methylation sites demonstrated the reliability of the data. Further, we performed DMR analysis using the Bumphunter method of the R package ChAMP and identified a total of 961 DMRs, which were classified into hyper-MRs and hypo-MRs based on |value| > 0.1 **(Figure 2B)**. We also identified the corresponding 896 genes in the DMRs. The hyper-MRs contained a total of 480 genes (hyper-MR-gene; **Supplementary Table 4**) and the hypo-MRs included 436 genes (hypo-MR-gene; **Supplementary Table 5**), of which 20 genes were hypermethylated and hypomethylated in different regions. We then mapped DMRs to the entire genome by creating an UpSet map and found that both hyper- **(Figure 2C)** and hypo- **(Figure 2D)** -MR-genes were mainly concentrated in TSS200, TSS1500, and body.

To investigate more closely the potential regulatory mechanisms of aberrant DNA methylation in psoriasis, we performed a functional enrichment analysis of the hyper-MR- and hypo-MR genes, respectively. GO analysis showed that the hyper-MR-genes were mainly enriched in the skeletal system ('embryonic skeletal system development', 'embryonic skeletal system morphogenesis', and 'skeletal system morphogenesis'; BP), 'pancreatic juice secretion' (BP), 'body fluid secretion' (BP), and MHC-related terms ['MHC class II protein complex' (CC), 'MHC protein complex' (CC), and 'MHC class II receptor activity' (MF)] **(Figure 3A; Supplementary Table 6)**. GO analysis of hypo-MR-genes **(Figure 3C; Supplementary Table 7)** indicated that in the BP category, these genes were tightly correlated with tissue/organ development ('embryonic organ development', 'gland development', 'sensory organ morphogenesis', *etc.*), immune response ('positive regulation of immune effector process', 'regulation of adaptive immune response', 'regulation of adaptive immune response based on somatic recombination of immune receptors built from immunoglobulin superfamily domains', *etc.*), immune cell biological processes ('T cell activation', 'positive regulation of leukocyte activation', 'B cell proliferation', *etc.*), cell cycle ('cell cycle G1/S phase transition', 'negative regulation of mitotic cell cycle phase transition', 'positive regulation of cell cycle', *etc.*), and apoptosis ('regulation of apoptotic signaling pathway', 'regulation of intrinsic apoptotic signaling pathway by p53 class mediator', 'negative regulation of intrinsic apoptotic signaling pathway by p53 class mediator', *etc.*); moreover, the 'regulation of cysteine-type endopeptidase activity', 'positive regulation of cysteine-type endopeptidase activity', 'molting cycle', and 'molting cycle process' were also significantly enriched. In the CC category, 'MHC protein complex', 'MHC class II protein complex', and 'lumenal side of membrane' were the three most

enriched terms. Moreover, a total of four MF terms, 'peptide antigen binding', 'DNA-binding transcription activator activity', 'DNA-binding transcription activator activity, RNA polymerase II-specific', and 'MHC class II protein complex binding' were enriched. KEGG analysis demonstrated that hyper-DEMR-genes enriched only 1 pathway, 'Cell adhesion molecules' **(Figure 3B; Supplementary Table 8)**; whereas hypo-MR-genes enriched a total of 35 KEGG pathways, including multiple diseases ('Type I diabetes mellitus', 'Autoimmune thyroid disease', 'Inflammatory bowel disease', *etc.*), viral infections ('Epstein-Barr virus infection', 'Human T-cell leukemia virus 1 infection', 'Influenza A', *etc.*), inflammatory responses ('Allograft rejection', 'Graft-versus-host disease', 'Antigen processing and presentation', *etc.*), immune cells ('Th1 and Th2 cell differentiation', 'Natural killer cell mediated cytotoxicity', 'Th17 cell differentiation', *etc.*), and apoptosis ('p53 signaling pathway', 'Apoptosis', 'TGF-beta signaling pathway', *etc.*) **(Figure 3D; Supplementary Table 10)**.

3.3 Identification and analysis of key differentially expressed methylation genes

To obtain differentially expressed methylated genes, we performed an overlap analysis of 767 psoriasis-related DEGs and 896 DMR-genes obtained above **(Figure 4A and B)**. Thirteen common genes were identified in the list of down-regulated DEGs and hyper-DMR-genes **(Figure 4A)**, namely TRIM2, HOXB3, TNXB, C1QTNF7, ESR1, CFL2, CCND1, DIXDC1, HLA-DQB2, PRLR, MACROD2, RORA, and ZSCAN18, which were termed as hyper-down-regulated genes; while there were 20 common genes in the list of up-regulated DEGs and hypo-DMR-genes **(Figure 4B)**, namely TAP1, S100A9, EPSTI1, GJB2, GRHL3, TTC22, SOX7, WNT5A, XAF1, GJB6, LAD1, POLR3G, KPNA2, E2F8, MX1, LTF, EPHX3, LGALS3BP, NUSAP1, and ESRP2, defined as hypo-up-regulated genes. The above-acquired genes were collectively labeled as differentially expressed methylation genes.

Subsequently, we constructed a PPI network for the above 33 differentially expressed methylated genes by STRING online analysis tool. After removing discrete nodes (confidence = 0.15), a PPI network was obtained for a total of 30 genes **(Figure 4C)**, which contained 61 edges. Based on the descending order of the degree values of each node, 10 key genes were identified, namely CCND1 (degree = 11), ESR1 (degree = 10), MX1 (degree = 9), WNT5A (degree = 8), LGALS3BP (degree = 8), GRHL3 (degree = 6), NUSAP1 (degree = 5), GJB2 (degree = 5), KPNA2 (degree = 5), and EPSTI (degree = 5), and the complex interactions between them were displayed in **Figure 4D**.

3.4 GJB2 was a diagnostic indicator for psoriasis

To obtain reliable and robust biomarkers and to reduce the possibility of overfitting, we employed three machine learning methods in the GSE13355 dataset, including LASSO regression, RF, and SVM-RFE for three-pass authentication. The optimal value of λ was set at 0.3958 based on the minimum criterion for LASSO regression, at which point one predictive feature (GJB2) with a non-zero coefficient was identified among the 10 key genes **(Figure 5A)**. The importance of each feature in the RF model was illustrated in **Figure 5B**, and after calculating the accuracy of the model under

different features using 10-fold cross-validation, it was determined that the model was most accurate when GJB2 was selected. In SVM-RFE, the accuracy of each combination of iterations was calculated by 10-fold cross-validation, which revealed that the SVM model appeared to have the best prediction performance when the first three genetic features (GJB2, WNT5A, and KPNA2) were included **(Figure 5C)**. Then, the potential feature genes obtained by the three algorithms were subjected to intersection analysis, and finally, the overlapping gene, GJB2, was identified as the hub gene for psoriasis **(Figure 5D)**.

Next, we evaluated the expression pattern of GJB2 between healthy control skin and lesioned skin samples from psoriasis patients by Wilcoxon rank-sum test in the GSE13355 and GSE14905 datasets. The results were presented in **Figures 6A and B**, where GJB2 was significantly overexpressed in psoriatic lesioned skin samples compared to healthy control skin samples (all $P < 0.0001$). Moreover, we assessed the DNA methylation levels of GJB2 between normal and psoriasis groups in GSE73894, the result showed that the DNA methylation levels of GJB2 were significantly lower in the psoriasis group **(Figure 6C)**. Further, ROC curves indicated that GJB2 was able to effectively differentiate between psoriatic samples and healthy control samples both in the GSE13355 dataset and in the GSE14905 dataset, with an AUC of 1 in the GSE13355 dataset **(Figure 6D)** and an AUC of 0.965 in the GSE14905 dataset **(Figure 6E)**. This evidence suggested that GJB2 was a potential diagnostic marker for psoriasis.

3.5 Single gene GSEA of GJB2

To further explore the potential molecular mechanisms of hub gene involvement in the psoriasis process, we performed a single-gene GSEA of GJB2 by R package clusterProfiler. The top 10 enriched terms from GO analysis were demonstrated in **Figure 7A**, all of which were in the BP category and closely associated with immune response (‘ACTIVATION OF IMMUNE RESPONSE’, ‘ACTIVATION OF INNATE IMMUNE RESPONSE’, and ‘ADAPTIVE IMMUNE RESPONSE’), antigen processing (‘ANTIGEN PROCESSING AND PRESENTATION’, ‘ANTIGEN PROCESSING AND PRESENTATION OF EXOGENOUS’, ‘PEPTIDE ANTIGEN VIA MHC CLASS I’, ‘ANTIGEN PROCESSING AND PRESENTATION OF PEPTIDE ANTIGEN’, ‘ANTIGEN PROCESSING AND PRESENTATION OF PEPTIDE ANTIGEN VIA MHC CLASS I’, and ‘ANTIGEN RECEPTOR MEDIATED SIGNALING PATHWAY’), ‘ANAPHASE PROMOTING COMPLEX DEPENDENT CATABOLIC PROCESS’, and ‘ATP METABOLIC PROCESS’. Besides, GJB2 was also notably linked to cell cycle (‘CELL CYCLE G2 M PHASE TRANSITION’, ‘DNA REPLICATION’, ‘MITOTIC NUCLEAR DIVISION’, *etc.*), tissue/organ growth and development (‘KIDNEY EPITHELIUM DEVELOPMENT’, ‘RENAL TUBULE DEVELOPMENT’, ‘SKELETAL SYSTEM MORPHOGENESIS’, *etc.*), and inflammatory response (‘INTERLEUKIN 1 BETA PRODUCTION’, ‘POSITIVE REGULATION OF CELL CELL ADHESION’, ‘INTERLEUKIN 6 PRODUCTION’). More importantly, some terms related to skin development were also significantly enriched, such as ‘REGULATION OF CYSTEINE TYPE ENDOPEPTIDASE ACTIVITY’, ‘KERATINOCYTE

DIFFERENTIATION', 'KERATINIZATION', 'EPIDERMIS DEVELOPMENT', and 'REGULATION OF MORPHOGENESIS OF AN EPITHELIUM' **(Supplementary Table 10)**. KEGG analysis showed that GJB2 was significantly associated with a variety of diseases ('ALZHEIMERS DISEASE', 'HUNTINGTONS DISEASE', 'PARKINSONS DISEASE', *etc.*), cell biological processes ('CELL CYCLE', 'DNA REPLICATION', 'P53 SIGNALING PATHWAY', 'TGF BETA SIGNALING PATHWAY', 'JAK STAT SIGNALING PATHWAY', *etc.*), and immune/inflammatory response ('ANTIGEN PROCESSING AND PRESENTATION', 'ALLOGRAFT REJECTION', 'PRIMARY IMMUNODEFICIENCY', 'CYTOKINE CYTOKINE RECEPTOR INTERACTION', *etc.*) related pathways **(Figure 7B; Supplementary Table 11)**. This evidence suggested that GJB2 may be involved in the development and progression of psoriasis by disrupting the body's immune system, mediating the cell cycle, and destroying the skin barrier, in addition to possibly inducing diseases related to the skeletal aspects of psoriasis, such as arthritic psoriasis, or being critical in the process of skeletal aberrations in patients with psoriasis treated with hormonal therapy.

3.6 Prediction of potential drugs targeting GJB2

GO-BP enrichment analysis revealed that GJB2 was inextricably linked to 'PTERIDINE CONTAINING COMPOUND METABOLIC PROCESS', 'PTERIDINE CONTAINING COMPOUND BIOSYNTHETIC PROCESS', and 'TETRAHYDROFOLATE METABOLIC PROCESS' **(Supplementary Table 10)**. Drugs commonly used in psoriasis, such as methotrexate, have been reported to restore the normal methylation state by interfering with the methyl transfer function of folic acid [40]. Inspired by this, we believed that GJB2 was most likely a hopeful therapeutic target to be developed for psoriasis. Using the DGIdb database, we predicted the interaction of GJB2 with molecular drugs, and a total of 2 compounds were put forward as inhibitors of GJB2, namely OCTANOL and CARBENOXOLONE **(Table 2)**. These drugs have the potential to become effective anti-psoriasis drugs in the future.

3.7 Relatively high expression of GJB2 in psoriasis

To further investigate the expression of GJB2 in psoriasis, we performed IHC staining and real-time qPCR using 8 psoriasis lesions and 11 healthy skin tissues. Just as we expected, IHC staining suggested that the protein level of GJB2 (connexin 26) was markedly higher in psoriasis lesions than in healthy controls **(Figure 8A, 8B and 8D)**. Moreover, the result of real-time qPCR indicated that the mRNA expression of GJB2 in psoriasis lesions is up-regulated compared to healthy controls **(Figure 8C)**.

4. Discussion

Identifying molecular targets and regulatory mechanisms related to DNA methylation would contribute to the diagnosis and treatment of psoriasis. In this study, we identified 767 psoriasis-related DEGs and 896 DMR-genes in various GEO databases. Thirty hyper-down-regulated genes and twenty hypo-up-regulated genes were screened by overlap analysis. About 10 key genes were constructed by the PPI network and GJB2 was finally identified the hug gene through filtered by multiple

machine learning algorithms. At the same time, we conducted a single-gene GSEA of GJB2. The result suggested that it might be involved in the development and progression of psoriasis by disrupting the body's immune system, mediating the cell cycle, and destroying the skin barrier. To verify the results of bioinformatics data analysis, we used the external dataset and qPCR to detect the expression of GJB2 in psoriasis.

GJB2 gene is located in the 13q11-12 region, with a total length of 5.5kb, encoding gap junction protein connexin 26(Cx26) [41]. Gap junction channels allow the exchange of ions, second messengers, and metabolites less than 1 kDa between adjacent cells, which acts a significant role in regulating homeostasis and tissue differentiation [42]. Screening gene mutation of GJB2 would contribute to gene diagnosis and genetic counseling in families with Non-Syndromic Hearing Loss (NSHL) [43]. Connexin 26 missense mutation resulting in palmoplantar keratoderma associated with sensorineural hearing loss [44]and temporal bones with cochlear otosclerosis [45]. The above diseases are largely caused by the thickening of the skin epidermis, which reveals a critical pattern for Cx26 in maintaining the balance between proliferation and differentiation of the epidermis.

Previous studies have found that the polymorphism of the GJB2 gene and the high expression of Cx26 is strongly correlated with the pathogenesis of psoriasis. Consistent with the experimental results of our study, the expression of Cx26 in psoriatic plaque was significantly up-regulated. Moreover, the high expression of Cx26 would destroy the skin barrier [46]and activate the skin inflammatory response [47]. Our single-gene GSEA also suggested that GJB2 may be involved in the development and progression of psoriasis by regulating the immune microenvironment of skin and destroying the skin barrier. Rs72474224 [48]and Rs3751385 [49] in GJB2 were preferentially associated with psoriasis susceptibility of the Chinese Han population.

We predict that octanol and carbenoxolone might be used as two new GJB2 inhibitors through the DGIdb database. Octanol is a kind of saturated fatty alcohol, which also acts as a T-type calcium channels (T-channels) inhibitor [50]. At present, there is no report on the application of octanol in the field of biomedicine. The therapeutic value of carbenoxolone has been proved in various diseases. Carbenoxolone could restrain the growth of colon cancer by blocking the gap junction channel and reducing the transport of glucose [51]. In angiotensin II-dependent hypertension, carbenoxolone combination with ramipril could significantly inhibit the proliferation and migration of VSMCs [52]. In addition, carbenoxolone would also exert an antiepileptic effect in vivo and in vitro by regulating gap junctions between astrocytes [55]. However, the application of carbenoxolone in psoriasis remains to be further studied.

This study indicated that GJB2 was a key gene for the diagnosis and treatment of psoriasis through combined multiomics, and single-gene GSEA revealed that GJB2 might induce psoriasis by regulating body immunity and destroying skin barrier. However, it also had some limitations. For example, the GEO database only generally divides the group into psoriasis or health, which lacks subdivision of disease subtypes and severity, and there is a certain heterogeneity between patients. In summary, our

study suggested that reversing the hypomethylation of GJB2 might be a new strategy for the treatment of psoriasis in the future.

5. Conclusions

In this study, we found that the abnormal expression of GJB2 could act a critical role in psoriasis development and progression. GJB2 might induce psoriasis by disrupting the body's immune system, mediating the cell cycle, and destroying the skin barrier. It would serve as a diagnostic indicator and therapeutic target in psoriasis.

6. Declarations

Abbreviations

Gap junction beta 2(GJB2), Tumor Immune Estimation Resource (TIMER), Gene Expression Omnibus (GEO), Single-gene gene set enrichment analysis (GSEA), Tumor Immune Dysfunction and Exclusion (TIDE) , Protein-protein interaction (PPI), differentially expressed genes (DEGs), least absolute shrinkage and selection operator (LASSO), Random Forest (RF), Support Vector Machine (SVM), Receiver operating characteristic (ROC), Genes and Genomes (KEGG), Drug-gene interaction database (DGIdb), Robust Multichip Average (RAM)

Ethics approval and consent to participate

Written informed consent was obtained from all participating patients prior to enrollment into the study. Study protocols were approved by the Ethics Committee of Kunming Children's Hospital, based on the ethical principles for medical research involving human subjects of the Helsinki Declaration.

Consent for publication

Not applicable.

Availability of data and material

The data underlying this study are freely available from(GSE13355; https://www.ncbi.nlm.nih.gov/geo/query/acc.cgi?acc=GSE13355),GSE14905(https://www.ncbi.nlm.nih.gov/geo/query/acc.cgi?acc=GSE14905) and GSE73894 (GPL13534 platform; https://www.ncbi.nlm.nih.gov/geo/query/acc.cgi?acc=GSE73894).

Competing interests

The authors declare that they have no competing interests.

Funding

This work was supported by grants from Kunming Science and technology planning project (No.2017-1-s-16248).

Authors' contributions

LX and SH designed the article. LY and NZ collected the specimen and conducted the experiment. ZZ and YP drafted the manuscript and were responsible for the acquisition of data. JW performed the statistical analysis. All authors read and approved the manuscript and agree to be accountable for all aspects of the research in ensuring that the accuracy or integrity of any part of the work are appropriately investigated and resolved.

Acknowledgements

Not applicable.

7. Reference

1.Boehncke WH, Schön MP. Psoriasis. Lancet. 2015;386(9997):983-994. doi:10.1016/S0140-6736(14)61909-7.

2.Parisi R, Iskandar IYK, Kontopantelis E, Augustin M, Griffiths CEM, Ashcroft DM. National, regional, and worldwide epidemiology of psoriasis: systematic analysis and modelling study. BMJ 2020; 369: m1590.

3.Parisi R, Symmons DP, Griffiths CE, Ashcroft DM; Identification and Management of Psoriasis and Associated ComorbidiTy (IMPACT) project team. Global epidemiology of psoriasis: a systematic review of incidence and prevalence. J Invest Dermatol. 2013;133(2):377-385. doi:10.1038/jid.2012.339

4.Michalek IM, Loring B, John SM. A systematic review of worldwide epidemiology of psoriasis. J Eur Acad Dermatol Venereol. 2017;31(2):205-212. doi:10.1111/jdv.13854.

5.Griffiths CEM, Armstrong AW, Gudjonsson JE, Barker JNWN. Psoriasis. Lancet. 2021;397(10281):1301-1315. doi:10.1016/S0140-6736(20)32549-6.

6.Rendon A, Schäkel K. Psoriasis Pathogenesis and Treatment. Int J Mol Sci. 2019;20(6):1475. Published 2019 Mar 23. doi:10.3390/ijms20061475.

7.Egeberg A, Ottosen MB, Gniadecki R, et al. Safety, efficacy and drug survival of biologics and biosimilars for moderate-to-severe plaque psoriasis. Br J Dermatol. 2018;178(2):509-519. doi:10.1111/bjd.16102.

8.Kamata M, Tada Y. Safety of biologics in psoriasis. J Dermatol. 2018;45(3):279-286. doi:10.1111/1346-8138.14096.

9.Kim HJ, Lebwohl MG. Biologics and Psoriasis: The Beat Goes On. Dermatol Clin.

2019;37(1):29-36. doi:10.1016/j.det.2018.07.004.

10.Ceccarelli M, Venanzi Rullo E, Berretta M, et al. New generation biologics for the treatment of psoriasis and psoriatic arthritis. State of the art and considerations about the risk of infection. Dermatol Ther. 2021;34(1):e14660. doi:10.1111/dth.14660.

11.Roszkiewicz M, Dopytalska K, Szymańska E, Jakimiuk A, Walecka I. Environmental risk factors and epigenetic alternations in psoriasis. Ann Agric Environ Med. 2020;27(3):335-342. doi:10.26444/aaem/112107.

12.Liu Y, Cui S, Sun J, Yan X, Han D. Identification of Potential Biomarkers for Psoriasis by DNA Methylation and Gene Expression Datasets. Front Genet. 2021;12:722803. Published 2021 Aug 26. doi:10.3389/fgene.2021.722803.

13.Whyte JM, Ellis JJ, Brown MA, Kenna TJ. Best practices in DNA methylation: lessons from inflammatory bowel disease, psoriasis and ankylosing spondylitis. Arthritis Res Ther. 2019;21(1):133. Published 2019 Jun 3. doi:10.1186/s13075-019-1922-y.

14.Robertson KD. DNA methylation and human disease. Nat Rev Genet. 2005;6(8):597-610. doi:10.1038/nrg1655.

15.Gu T, Goodell MA. The push and pull of DNA methylation. Science. 2021;372(6538):128-129. doi:10.1126/science.abh3187.

16.Chatterjee R, Vinson C. CpG methylation recruits sequence specific transcription factors essential for tissue specific gene expression. Biochim Biophys Acta. 2012;1819(7):763-770. doi:10.1016/j.bbagrm.2012.02.014.

17.Zlotorynski E. Epigenetics: DNA methylation prevents intragenic transcription. Nat Rev Mol Cell Biol. 2017;18(4):212-213. doi:10.1038/nrm.2017.25

18.Bai J, Liu Z, Xu Z, et al. Epigenetic downregulation of SFRP4 contributes to epidermal hyperplasia in psoriasis [J]. J Immunol,2015, 194(9):4185-4198.

19.Ruchusatsawat K, Thiemsing L, Mutirangura A, et al. BCAP 31 expression and promoter demethylation in psoriasis [J]. Asian Pac J Allergy Immunol, 2017, 35(2):86-90.

20.Zhang P, Zhao M, Liang G, et al. Whole-genome DNA methylation in skin lesions from patients with psoriasis vulgaris [J]. J Autoimmun, 2013, 41:17-24.

21.Gu X, Nylander E, Coates PJ, et al. Correlation between Reversal of DNA Methylation and Clinical Symptoms in Psoriatic Epidermis Following Narrow-Band UVB Phototherapy[J]. J Invest Dermatol,2015, 135(8):2077-2083.

22.Nair RP, Duffin KC, Helms C, et al. Genome-wide scan reveals association of psoriasis with IL-23 and NF-kappaB pathways. Nat Genet. 2009;41(2):199-204. doi:10.1038/ng.311.

23.Swindell WR, Johnston A, Carbajal S, et al. Genome-wide expression profiling of five mouse models identifies similarities and differences with human psoriasis. PLoS One. 2011;6(4):e18266. Published 2011 Apr 4. doi:10.1371/journal.pone.0018266.

24.Ding J, Gudjonsson JE, Liang L, et al. Gene expression in skin and lymphoblastoid cells: Refined statistical method reveals extensive overlap in cis-eQTL signals. Am J Hum Genet. 2010 ;87(6):779-789. doi:10.1016/j.ajhg.2010.10.024.

25.Yao Y, Richman L, Morehouse C, et al. Type I interferon: potential therapeutic target for psoriasis? [published correction appears in PLoS ONE. 2009;4(3). doi: 10.1371/annotation /fbcbcab9-2e87-4ec7-af6e-c6e9e64ad4b3]. PLoS One. 2008;3(7):e2737. Published 2008 Jul 16. doi:10.1371/journal.pone.0002737.
26.Zhou F, Wang W, Shen C, et al. Epigenome-Wide Association Analysis Identified Nine Skin DNA Methylation Loci for Psoriasis. J Invest Dermatol. 2016;136(4):779-787. doi:10.1016/j.jid. 2015.12.029.
27.Shen C, Wen L, Ko R, et al. DNA methylation age is not affected in psoriatic skin tissue. Clin Epigenetics. 2018;10(1):160. Published 2018 Dec 27. doi:10.1186/s13148-018-0584-y.
28.Ritchie ME, Phipson B, Wu D, et al. limma powers differential expression analyses for RNA-sequencing and microarray studies. Nucleic Acids Res. 2015;43(7):e47. doi:10.1093/nar/gkv 007.
29.Conway JR, Lex A, Gehlenborg N. UpSetR: an R package for the visualization of intersecting sets and their properties. Bioinformatics. 2017;33(18):2938-2940. doi:10.1093/bioinformatics/btx 364.
30.The Gene Ontology Consortium. Expansion of the Gene Ontology knowledgebase and resources. Nucleic Acids Res. 2017;45(D1):D331-D338. doi:10.1093/nar/gkw1108.
31.Kanehisa M, Goto S. KEGG: kyoto encyclopedia of genes and genomes. Nucleic Acids Res. 2000;28(1):27-30. doi:10.1093/nar/28.1.27.
32.Yu G, Wang LG, Han Y, He QY. clusterProfiler: an R package for comparing biological themes among gene clusters. OMICS. 2012;16(5):284-287. doi:10.1089/omi.2011.0118.
33.Shannon P, Markiel A, Ozier O, et al. Cytoscape: a software environment for integrated models of biomolecular interaction networks. Genome Res. 2003;13(11):2498-2504. doi:10.1101/gr.12393 03.
34.Retraction [retraction of: Clin Oral Implants Res. 2012 Feb;23(2):236-244]. Clin Oral Implants Res. 2018;29(6):667. doi:10.1111/clr.13093.
35.Petkovic D, Altman R, Wong M, Vigil A. Improving the explainability of Random Forest classifier - user centered approach. Pac Symp Biocomput. 2018;23:204-215.
36.Huang ML, Hung YH, Lee WM, Li RK, Jiang BR. SVM-RFE based feature selection and Taguchi parameters optimization for multiclass SVM classifier. ScientificWorldJournal. 2014;2014:795624. doi:10.1155/2014/795624.
37.Robin X, Turck N, Hainard A, et al. pROC: an open-source package for R and S+ to analyze and compare ROC curves. BMC Bioinformatics. 2011;12:77. Published 2011 Mar 17. doi:10.1186 /1471-2105-12-77.
38.Wagner AH, Coffman AC, Ainscough BJ, et al. DGIdb 2.0: mining clinically relevant drug-gene interactions. Nucleic Acids Res. 2016;44(D1):D1036-D1044. doi:10.1093/nar/gkv1165.
39.Chandra A, Senapati S, Roy S, Chatterjee G, Chatterjee R. Epigenome-wide DNA methylation regulates cardinal pathological features of psoriasis. Clin Epigenetics. 2018;10(1):108. Published 2018 Aug 9. doi:10.1186/s13148-018-0541-9.
40.Kim YI, Logan JW, Mason JB, Roubenoff R. DNA hypomethylation in inflammatory arthritis: reversal with methotrexate. J Lab Clin Med. 1996;128(2):165-172. doi:10.1016/s0022-2143(96)90 008-6.
41.Garcia-Vega L, O'Shaughnessy EM, Albuloushi A, Martin PE. Connexins and the Epithelial Tissue Barrier: A Focus on Connexin 26. Biology (Basel). 2021;10(1):59. Published 2021 Jan 14.

doi:10.3390/biology10010059.
42.Beyer EC, Berthoud VM. Gap junction gene and protein families: Connexins, innexins, and pannexins. Biochim Biophys Acta Biomembr. 2018;1860(1):5-8. doi:10.1016/j.bbamem.2017.05.016.
43.Mishra S, Pandey H, Srivastava P, Mandal K, Phadke SR. Connexin 26 (GJB2) Mutations Associated with Non-Syndromic Hearing Loss (NSHL). Indian J Pediatr. 2018;85(12):1061-1066. doi:10.1007/s12098-018-2654-8.
44.Lam MW, Veitch D, Woo PN. Connexin 26 missense mutation resulting in syndromic hearing loss with palmoplantar keratoderma. Int J Dermatol. 2020;59(12):e454-e455. doi:10.1111/ijd.15139.
45.Miller ME, Lopez IA, Linthicum FH, Ishiyama A. Connexin 26 Immunohistochemistry in Temporal Bones With Cochlear Otosclerosis. Ann Otol Rhinol Laryngol. 2018;127(8):536-542. doi:10.1177/0003489418779410.
46.Garcia-Vega L, O'Shaughnessy EM, Albuloushi A, Martin PE. Connexins and the Epithelial Tissue Barrier: A Focus on Connexin 26. Biology (Basel). 2021;10(1):59. Published 2021 Jan 14. doi:10.3390/biology10010059.
47.García-Vega L, O'Shaughnessy EM, Jan A, Bartholomew C, Martin PE. Connexin 26 and 43 play a role in regulating proinflammatory events in the epidermis [published online ahead of print, 2019 Feb 2]. J Cell Physiol. 2019;10.1002/jcp.28206. doi:10.1002/jcp.28206.
48.Yao F, Yue M, Zhang C, et al. A genetic coding variant rs72474224 in GJB2 is associated with clinical features of psoriasis vulgaris in a Chinese Han population. Tissue Antigens. 2015;86(2):134-138. doi:10.1111/tan.12595
49.Liu QP, Wu LS, Li FF, et al. The association between GJB2 gene polymorphism and psoriasis: a verification study. Arch Dermatol Res. 2012;304(9):769-772. doi:10.1007/s00403-012-1273-x.
50.Akhtar MK, Dandapani H, Thiel K, Jones PR. Microbial production of 1-octanol: A naturally excreted biofuel with diesel-like properties. Metab Eng Commun. 2014;2:1-5. Published 2014 Nov 13. doi:10.1016/j.meteno.2014.11.001
51.Gong K, Hong Q, Wu H, et al. Gap junctions mediate glucose transfer to promote colon cancer growth in three-dimensional spheroid culture [published online ahead of print, 2022 Jan 28]. Cancer Lett. 2022;531:27-38. doi:10.1016/j.canlet.2022.01.023.
52.Gao RJ, Zhang AM, Jia QH, et al. The promoting role of Cx43 on the proliferation and migration of arterial smooth muscle cells for angiotensin II-dependent hypertension. Pulm Pharmacol Ther. 2021;70:102072. doi:10.1016/j.pupt.2021.102072.
53.Volnova A, Tsytsarev V, Ganina O, et al. The Anti-Epileptic Effects of Carbenoxolone In Vitro and In Vivo. Int J Mol Sci. 2022;23(2):663. Published 2022 Jan 8. doi:10.3390/ijms23020663.

Figure Legends:

Figure 1 Analysis of DEGs between psoriasis and healthy samples in the GSE13355 dataset. (A)Volcano plot of the 767 DEGs in the GSE13355 dataset. Red, upregulation; blue, downregulation. (B)Hierarchical clustering heatmap of the top 100 up- and down-DEGs between psoriasis and healthy samples. The higher and lower expressed genes were shown in red and green, respectively. (C)The top 10 GO-biological processes, cellular components, and molecular functions of 767 DEGs. (D)All 9 enriched KEGG pathways of the DEGs. Significantly enriched terms/pathways of DEGs are indicated in Y-axis. Rich factor in the X-axis represents the enrichment levels. The larger value of Rich factor represents the higher level of enrichment. The color of the dot stands for the different adjusted P-value and the size of the dot reflects the number of target genes enriched in the corresponding term/pathway.

Figure 2 DNA methylation profiling of healthy controls and psoriasis lesions in the GSE73894 database. (A)DNA methylation levels in healthy controls and psoriasis lesions. (B)Chromosome distribution of DMRs. The number of dots represents the distribution of DMR across different chromosomes. (C and D)Genomic distribution of the hyper-DMRs and hypo-DMRs. Pie charts represent the proportion of DMRs in different genomic contexts. Upset graphs represent the number of DMRs distributed in single or combined genomic regions.

Figure 3 Functional enrichment analysis of the hyper-MR- and hypo-MR genes. (A) GO analysis of hyper-MR-genes. (B)KEGG analysis of hyper-MR-genes. (C)GO analysis of hypo-MR genes. (D)KEGG analysis of hypo-MR genes.

Figure 4 Identification and analysis of key differentially expressed methylation genes. (A)Venn diagram shows the intersecting genes from down-regulated DEGs and hyper-DMR-genes. (B)The Venn graph shows intersection of up-regulated DEGs and hypo-DMR-genes.(C)Visualized PPI analysis of differentially expressed methylation genes.(D)Top 10 genes with the highest degree values in differentially expressed methylation genes, darker color represents higher degree values.

Figure 5 Identification of the hub gene. (A)Identification of feature gene by Least absolute shrinkage and selection operator(LASSO) regression analysis. The horizontal axis represents the lambda value and the vertical axis represents the independent variable coefficient. (B)Screen diagnostic markers by random forest (RF) model algorithm. The importance of features ranked by mean decrease Gini. (C)Selection genes by the support vector machine recursive feature elimination (SVM-RFE) algorithm. (D)Intersection analysis of feature genes identified by three algorithms.

Figure 6 Differential expression/methylation of GJB6 in samples and assessment of diagnostic value. (A)The expression of GJB2 between healthy controls and psoriasis lesions in the GSE13355 dataset. (B)The expression of GJB2 between healthy controls and psoriasis lesions in the GSE14905 dataset. (C)The DNA methylation levels of GJB2 between healthy controls and psoriasis lesions in the GSE73894 dataset. (D)The ROC curve of the GJB2 showing the sensitivity and specificity based on the GSE13355 dataset. (E)The ROC curve of the GJB2 showing the sensitivity and specificity based on the GSE14905 dataset.

Figure 7 GSEA enrichment analysis of GJB2 using the GSE13355 dataset. (A)The

top 10 enriched gene sets in GO system. (B)The top 10 enriched gene sets in KEGG collection. Each line representing one particular gene set with unique color. Only gene sets with |NES| > 1, P < 0.05, and q < 0.2 were considered significant.

Figure 8 GJB2 expression in healthy controls and psoriasis lesions. (A) Immunohistochemical staining of GJB2 protein in psoriasis lesions. (B) Immunohistochemical staining of GJB2 protein in healthy controls. (C)The relative expression of GJB2 in the psoriasis lesions samples (n = 8) collected in our hospital were detected using quantitative PCR (qPCR). GAPDH was used as an internal reference gene for normalization. Data were analyzed using un-paired Student's t-test.

Table Legends:

Table1 Primer sequence of GJB2 and GAPDH.

Table2 The inhibitory drugs of GJB2.

Figures

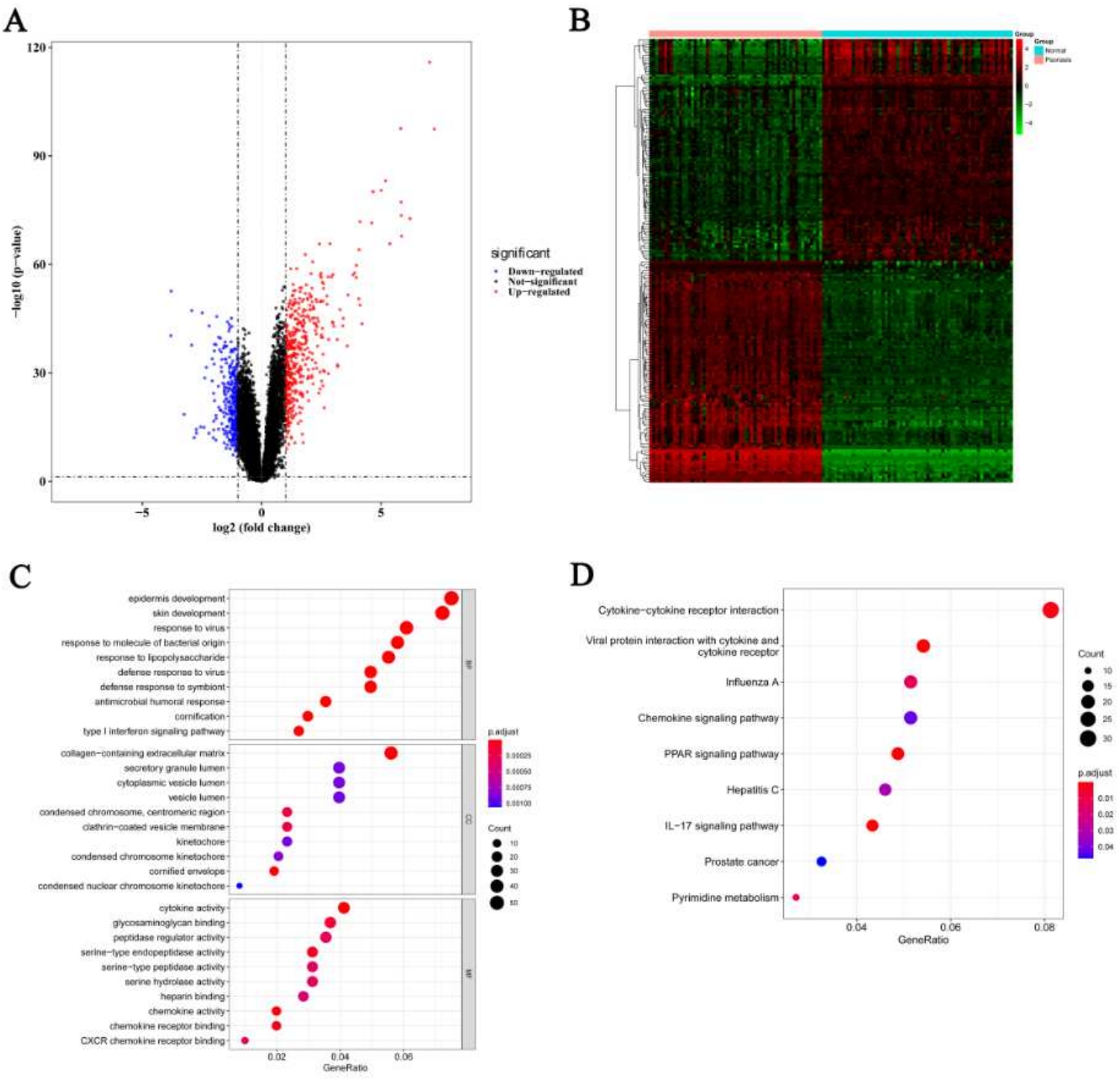

Figure 1

See manuscript for legend.

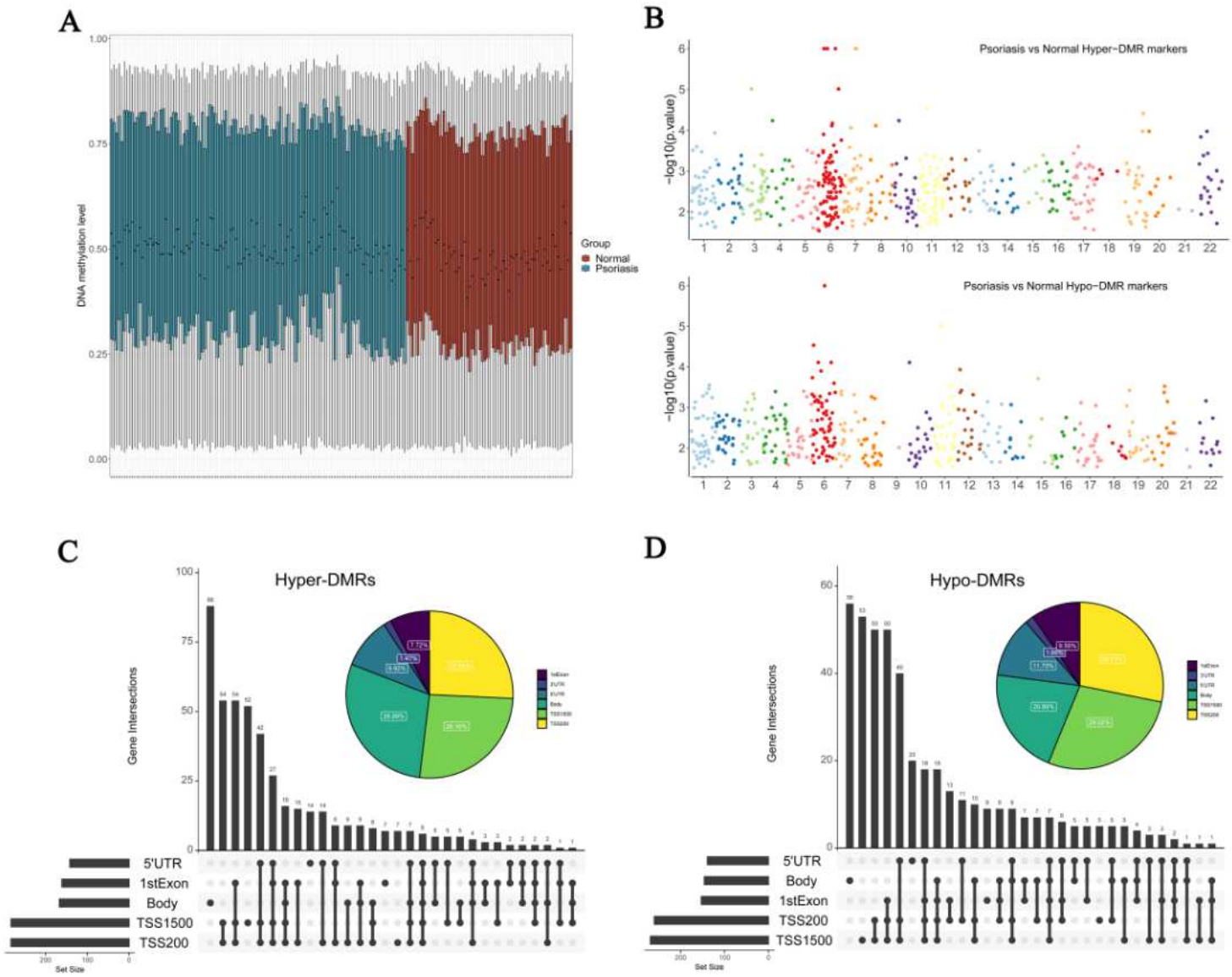

Figure 2

See manuscript for legend.

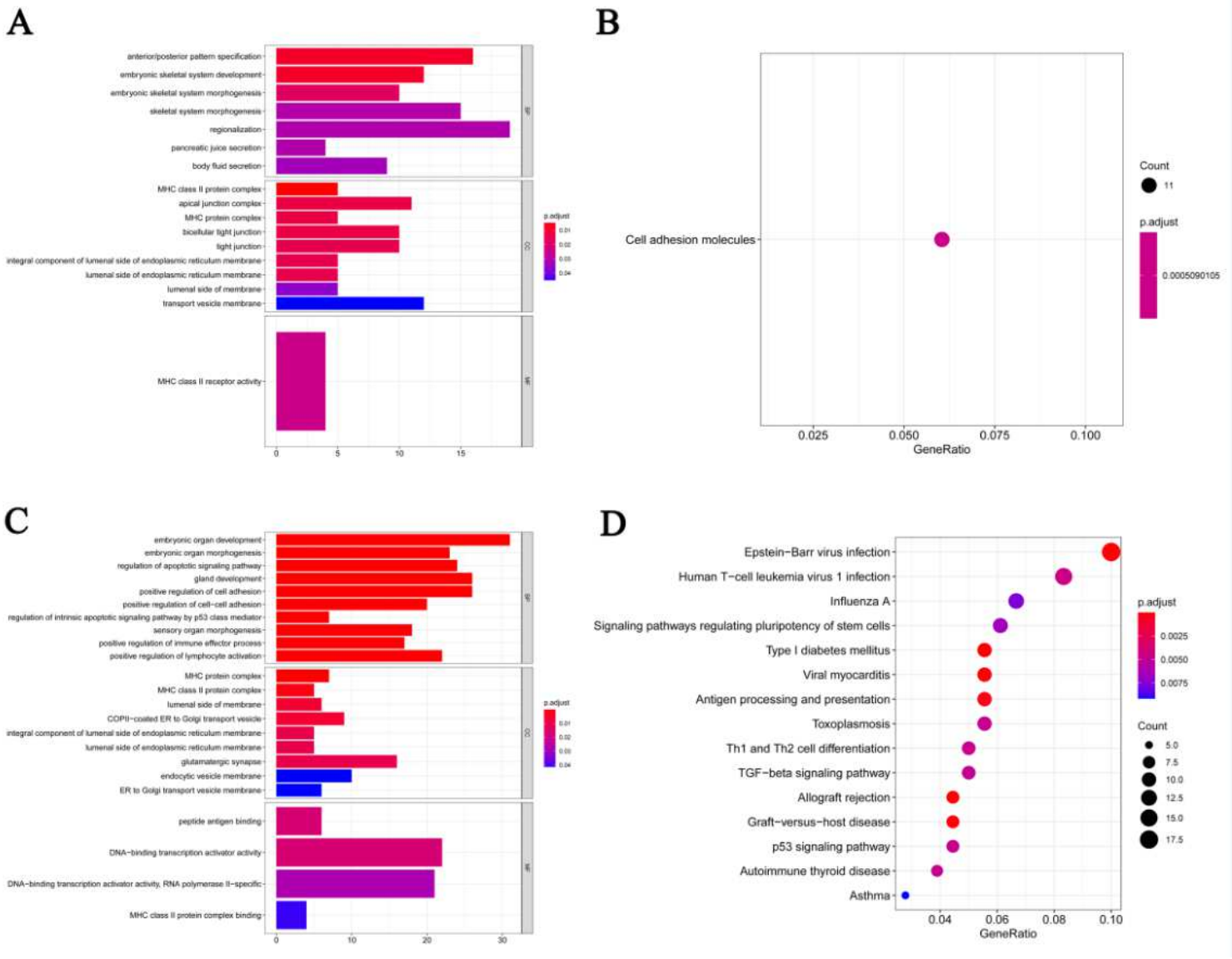

Figure 3

See manuscript for legend.

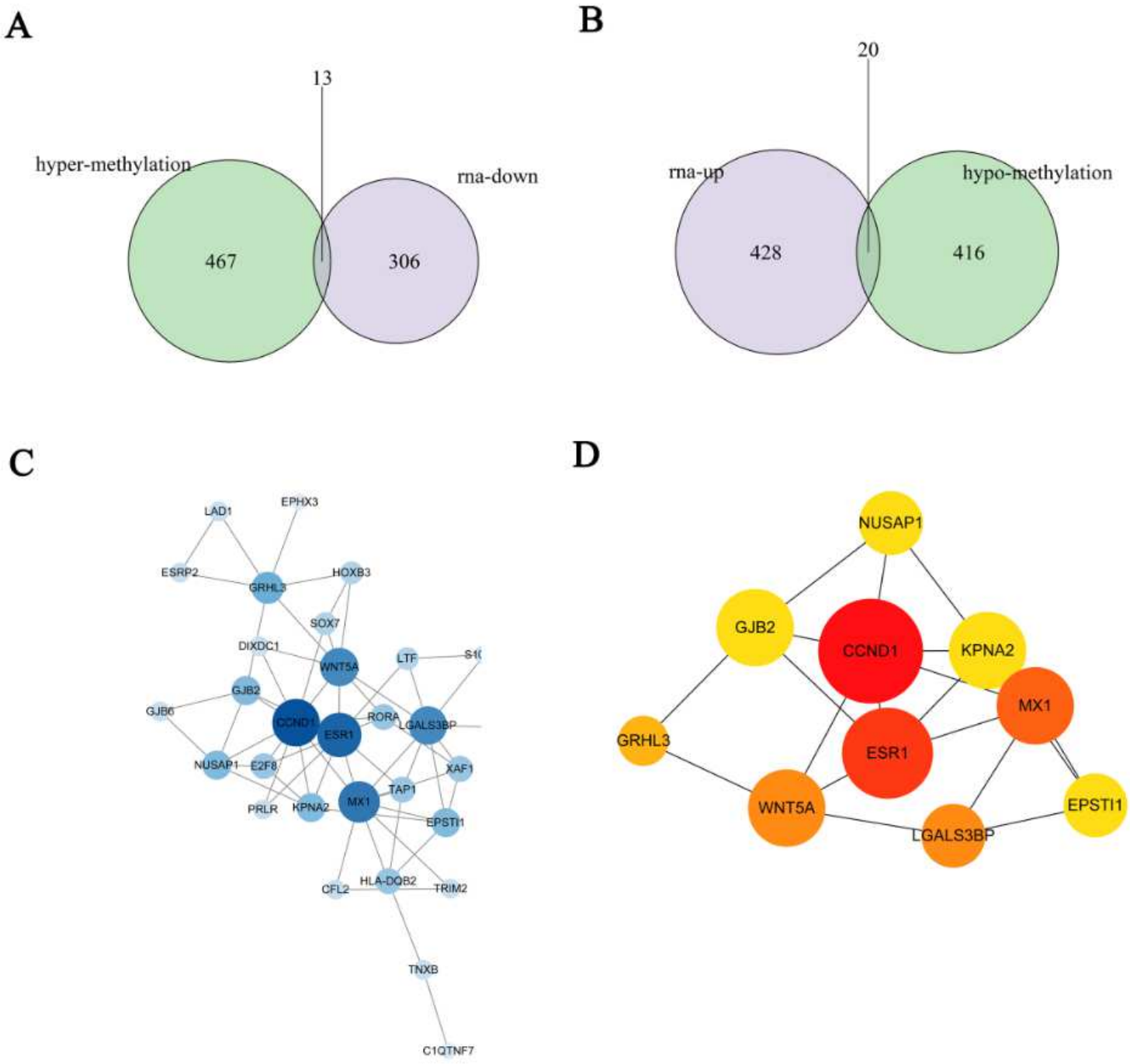

Figure 4

See manuscript for legend.

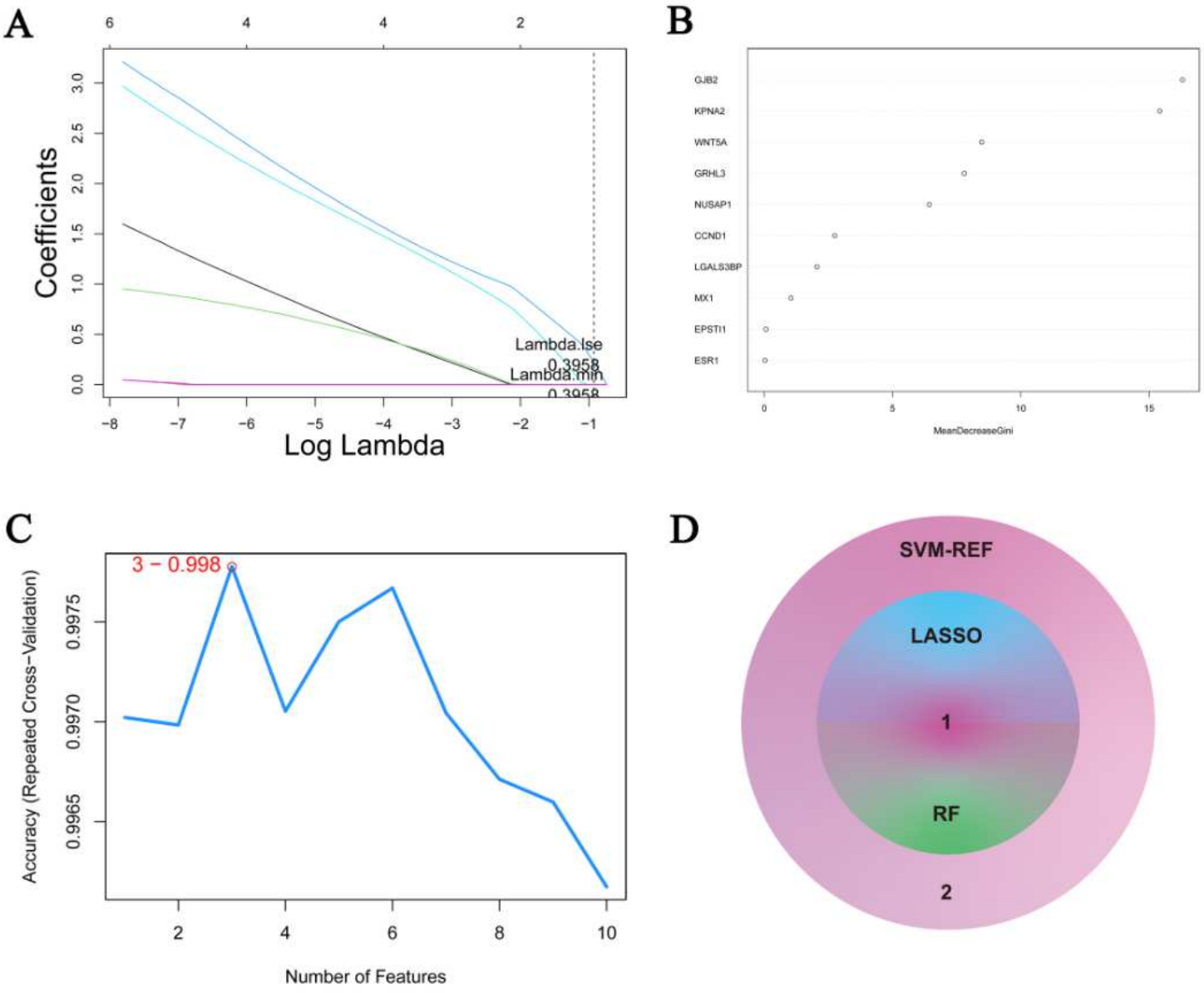

Figure 5

See manuscript for legend.

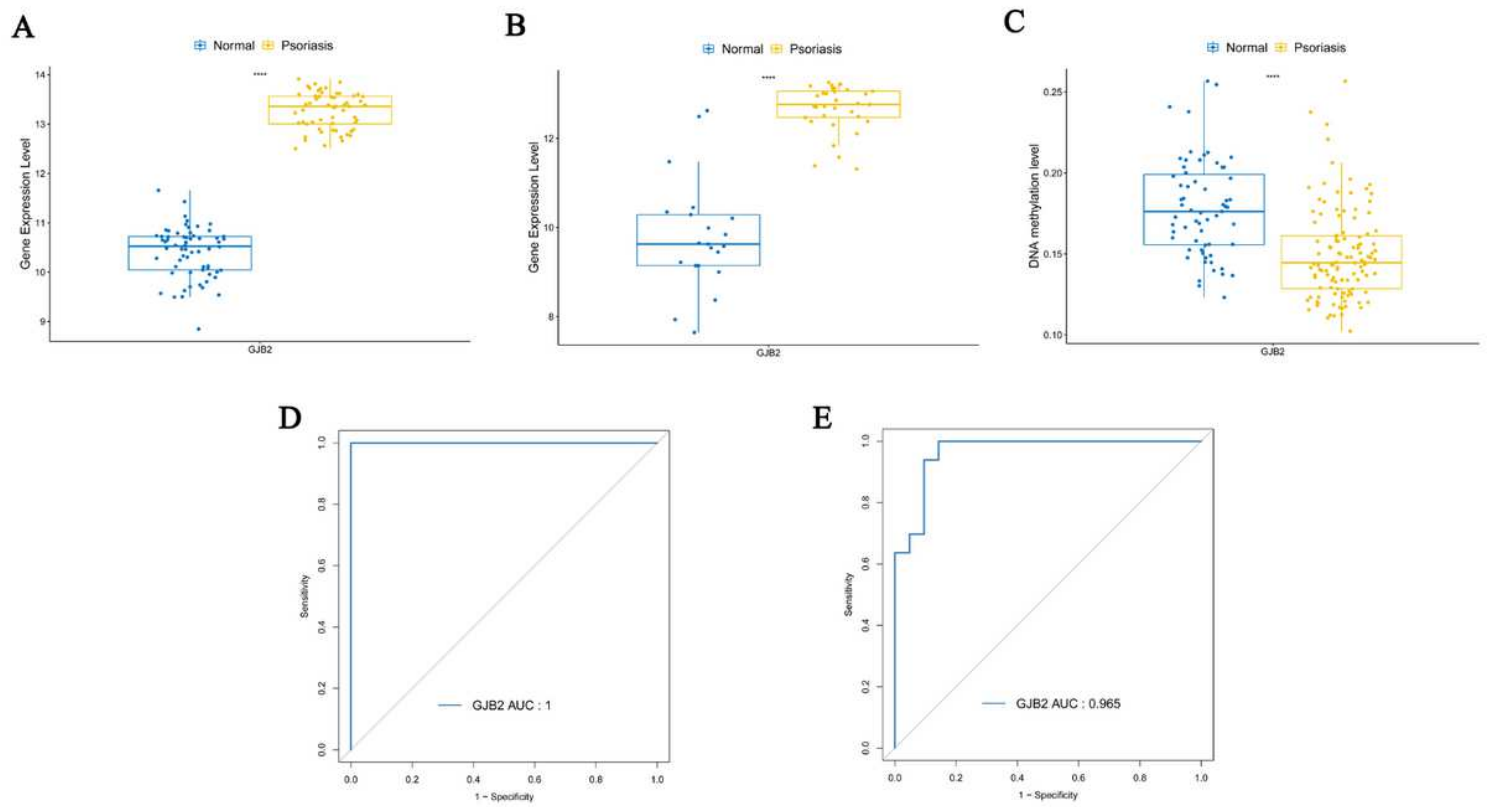

Figure 6

See manuscript for legend.

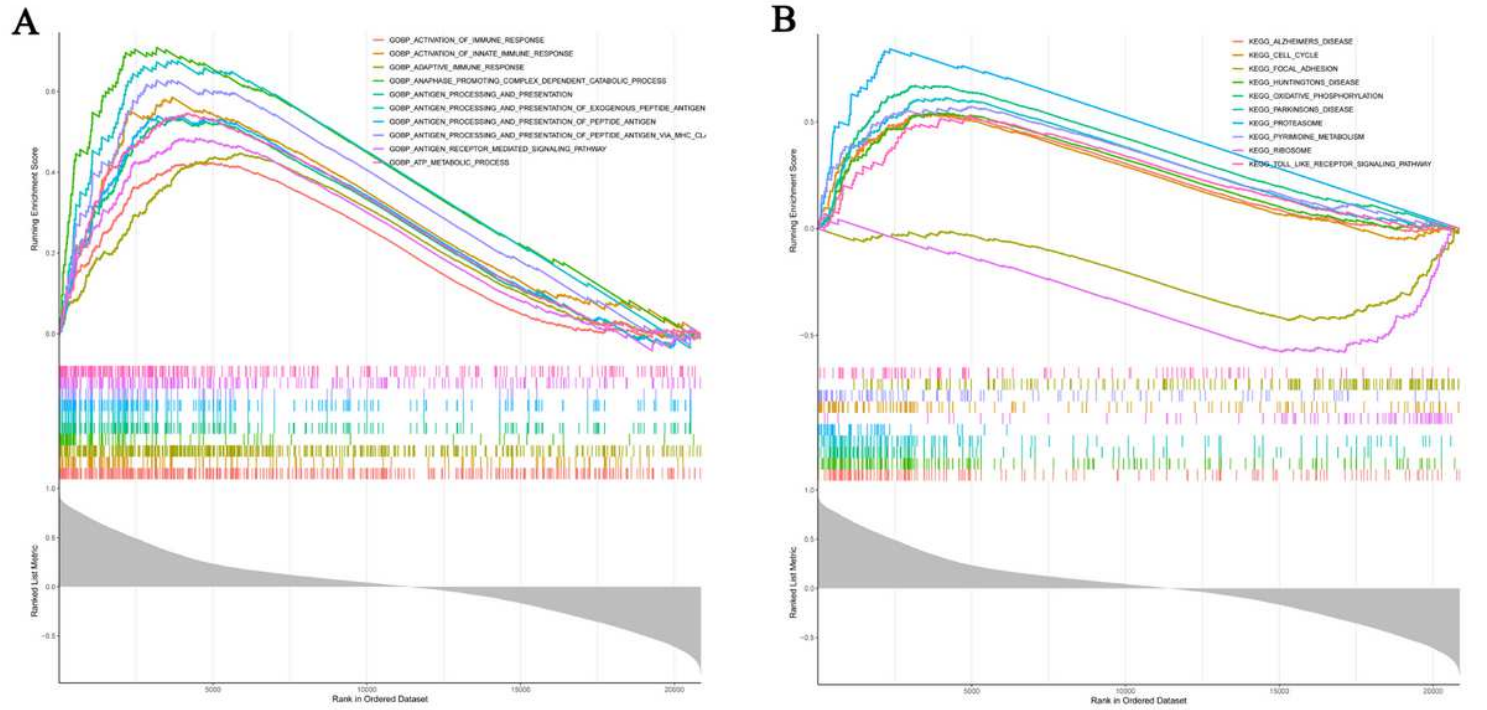

Figure 7

See manuscript for legend.

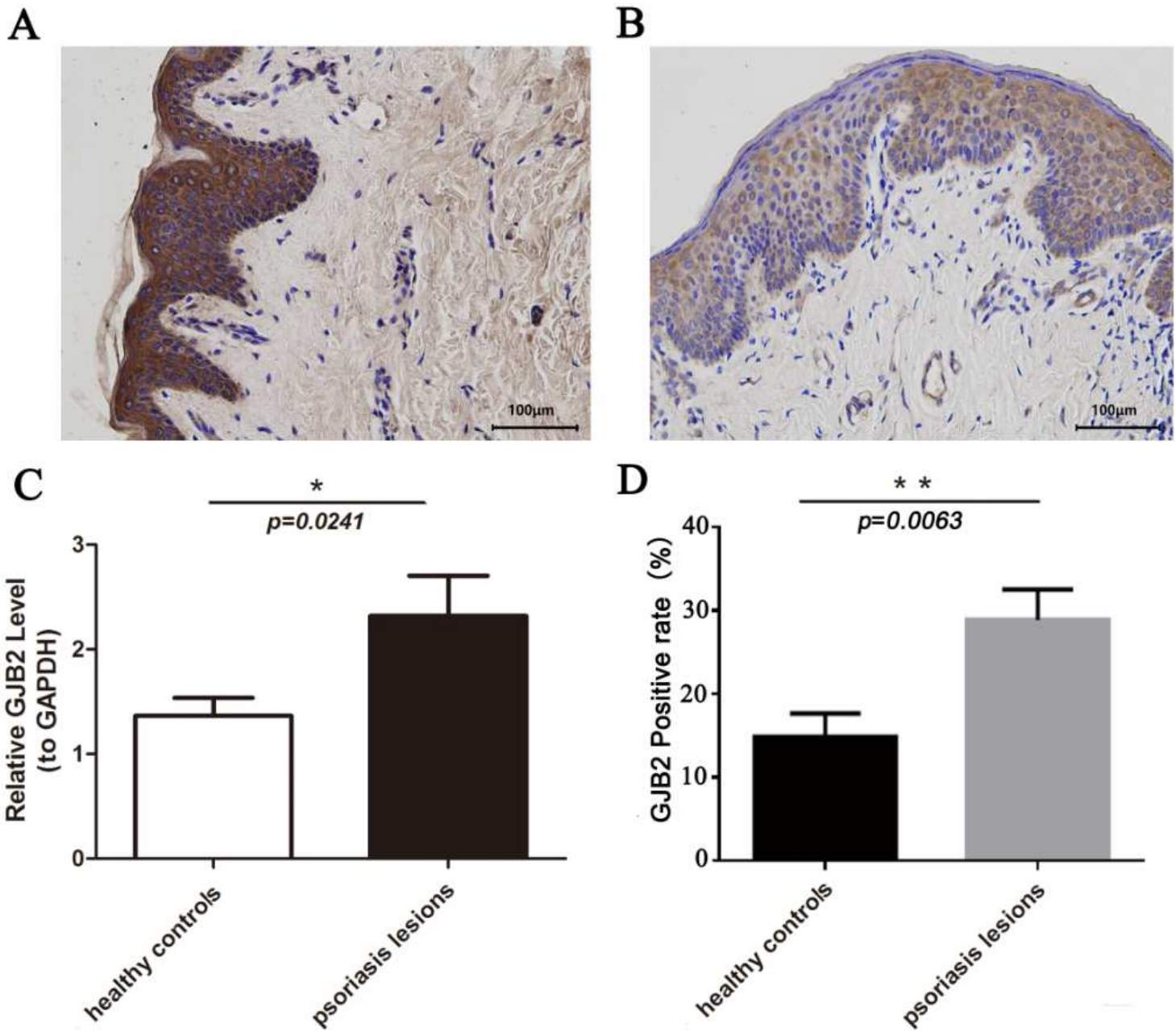

Figure 8

See manuscript for legend.

Supplementary Files

This is a list of supplementary files associated with this preprint. Click to download.

- SupplementaryFigure1.tif
- SupplementaryFigure2.tif
- SupplementaryTable1.xlsx
- SupplementaryTable2.xlsx

- SupplementaryTable3.xlsx
- SupplementaryTable4.xlsx
- SupplementaryTable5.xlsx
- SupplementaryTable6.xlsx
- SupplementaryTable7.xlsx
- SupplementaryTable8.xlsx
- SupplementaryTable9.xlsx
- SupplementaryTable10.xlsx
- SupplementaryTable11.xlsx